LETTERS
https://doi.org/10.1038/s41550-019-0779-y

nature astronomy

Molybdenum isotopic evidence for the late accretion of outer Solar System material to Earth

Gerrit Budde*, Christoph Burkhardt and Thorsten Kleine

Earth grew through collisions with Moon-sized to Mars-sized planetary embryos from the inner Solar System, but it also accreted material from greater heliocentric distances[1,2], including carbonaceous chondrite-like bodies, the likely source of Earth's water and highly volatile species[3,4]. Understanding when and how this material was added to Earth is critical for constraining the dynamics of terrestrial planet formation and the fundamental processes by which Earth became habitable. However, earlier studies inferred very different timescales for the delivery of carbonaceous chondrite-like bodies, depending on assumptions about the nature of Earth's building materials[5–11]. Here we show that the Mo isotopic composition of Earth's primitive mantle falls between those of the non-carbonaceous and carbonaceous reservoirs[12–15], and that this observation allows us to quantify the accretion of carbonaceous chondrite-like material to Earth independently of assumptions about its building blocks. As most of the Mo in the primitive mantle was delivered by late-stage impactors[10], our data demonstrate that Earth accreted carbonaceous bodies late in its growth history, probably through the Moon-forming impact. This late delivery of carbonaceous material probably resulted from an orbital instability of the gas giant planets, and it demonstrates that Earth's habitability is strongly tied to the very late stages of its growth.

Nucleosynthetic isotope anomalies arise from the heterogeneous distribution of isotopically anomalous stellar-derived matter in the accretion disk and, as such, are a powerful tool to determine the nature and origin of Earth's building material[8,10,16–18]. However, current models utilizing these isotope anomalies to reconstruct Earth's accretion history and the delivery time of carbonaceous chondrite-like material are uncertain[18], because they rely on the contested[8,16,17] assumption that known meteorites represent Earth's building material[8–11]. Here, we overcome this inherent uncertainty and present a new approach to this problem, which requires no assumptions about the isotopic composition of Earth's building material. Our approach uses the nucleosynthetic Mo isotope dichotomy between non-carbonaceous (NC) and carbonaceous (CC) meteorites, which represent two genetically distinct reservoirs that coexisted in the protoplanetary disk for several million years[12–15]. While the NC reservoir represents inner Solar System material, the CC reservoir was located at greater heliocentric distance, presumably beyond Jupiter's orbit[12,13,18], and includes carbonaceous chondrites, the likely source of Earth's water and highly volatile species[3,4]. Compared with NC meteorites, CC meteorites have an excess in nuclides produced in the rapid neutron capture process[12,13] (*r*-process) and possibly also the proton capture process[11,14] (*p*-process) of stellar nucleosynthesis. Additionally, meteorites from both groups exhibit variable abundances of Mo produced in the slow neutron capture process (*s*-process). Consequently, in a plot of ε^{94}Mo versus ε^{95}Mo (where ε^{i}Mo is the parts-per-10,000 deviation from a terrestrial Mo standard), NC and CC meteorites plot on two distinct *s*-process mixing lines (the NC and CC lines), where their offset reflects the *r*-process (and possibly *p*-process) excess of the CC reservoir (Fig. 1).

As Mo is a siderophile (iron-loving) element, most of the Mo in Earth's primitive mantle (hereafter referred to as bulk silicate Earth (BSE)) derives from the late stages of accretion, because Mo from earlier stages was largely removed into Earth's core[10]. Thus, if Earth received CC material only during early accretion stages, as proposed in previous studies[10,11], the BSE would plot on the NC line. Conversely, if Earth accreted CC material during the latest accretion stages, the BSE would plot off the NC line towards the CC line. However, current data[11–15] do not define the slope and intercept of the NC line or the BSE's Mo isotopic composition precisely enough to determine where the BSE plots.

We obtained Mo isotope data for many previously uninvestigated bulk meteorites, various terrestrial rock samples, and acid leachates from two primitive ordinary chondrites (Supplementary Table 1). The newly analysed bulk meteorites and the acid leachates plot on a single *s*-process mixing line together with enstatite and ordinary chondrites and several iron meteorites. The linear regression of the combined data is consistent with the NC line observed in previous studies[11–15] but is now more precisely defined (Fig. 1 and Supplementary Information). Importantly, the newly defined NC-line slope of 0.596 ± 0.008 is identical to the slope of the CC line (0.596 ± 0.006), and both are consistent with the slope determined from Mo isotope measurements of presolar mainstream SiC grains (0.59)[19]. The fact that the NC and CC lines are parallel indicates that the Mo isotopic variability along them comes from heterogeneous distribution of the same or similar *s*-process carrier(s), and that the CC reservoir contains a constant *r*-process excess over the NC reservoir. Thus, the processes leading to the *s*-process variations evidently did not affect the *r*-process material in the two reservoirs, suggesting that this *r*-process material is not contained in individual presolar carriers; instead, the constant *r*-process difference between the CC and NC reservoirs reflects a characteristic isotopic difference between two bulk disk reservoirs[20].

It has been proposed that during the Solar System's first few million years, the composition of the inner disk (that is, the NC reservoir) changed continuously by admixture of outer Solar System material (that is, CC-derived material)[9]. If so, then later-formed NC bodies (for example, ordinary chondrites) should exhibit an *r*-process excess compared with earlier-formed NC bodies (for example, group IC, IIAB, IIIAB, IVA iron meteorites)[13]. However, all NC meteorites plot on the NC line, indicating that they accreted from material with identical *r*-process proportions (Fig. 1). The NC–CC dichotomy, therefore, cannot reflect a secular change of inner disk composition[9], but instead results from efficient spatial separation of two genetically distinct source regions[12,13].

Institut für Planetologie, University of Münster, Wilhelm-Klemm-Straße 10, 48149 Münster, Germany. *e-mail: gerrit.budde@uni-muenster.de

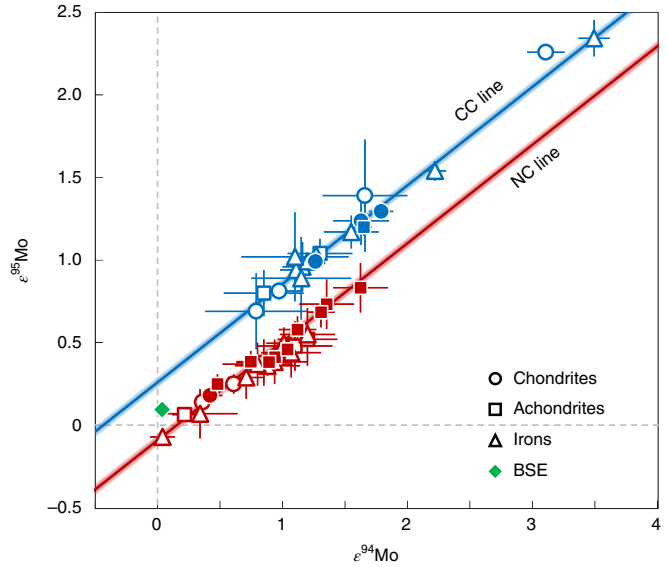

Fig. 1 | Mo isotope dichotomy of meteorites in ε^{95}Mo versus ε^{94}Mo space. Carbonaceous (CC, blue) and non-carbonaceous (NC, red) meteorites define two parallel lines with identical slopes. Samples from both groups show variable *s*-process deficits relative to the terrestrial standard ($\varepsilon^{95}\text{Mo} \equiv 0$, $\varepsilon^{94}\text{Mo} \equiv 0$), resulting in isotope variations along each line. The offset between the two lines results from a constant *r*-process excess in the CC reservoir. The BSE (green) plots between the NC and CC lines, demonstrating that the BSE's Mo derives from both the NC and CC reservoirs. Open symbols represent literature data (Supplementary Table 4), closed symbols are data from this study. Error envelopes and error bars typically represent 95% confidence intervals (95% CI).

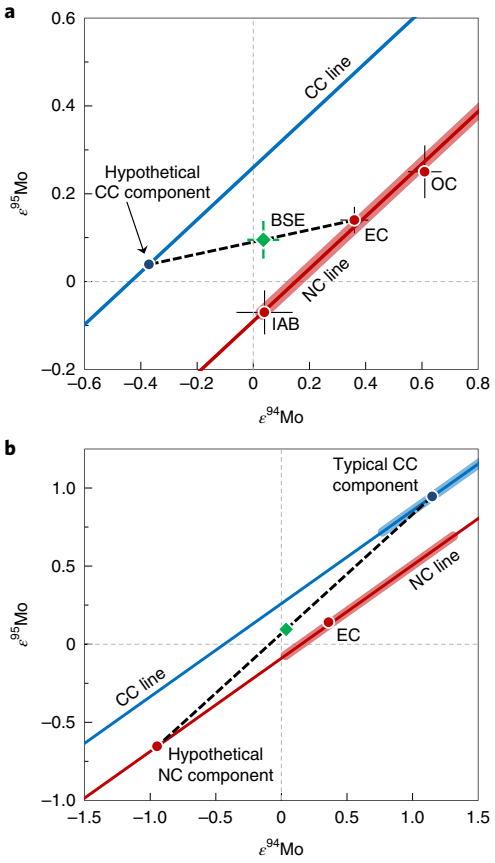

Fig. 2 | Two potential scenarios for reproducing the BSE's Mo isotopic composition. a, Mixing between EC-like material and presumed *s*-process-enriched CC material. **b**, Mixing between presumed *s*-process-enriched NC material and a CC component having a typical composition of carbonaceous meteorites ($\varepsilon^{94}\text{Mo} \approx 1.15$; $\varepsilon^{95}\text{Mo} \approx 0.95$). In both scenarios an unknown component with an *s*-process excess is required to balance the *s*-process deficit observed for known meteorites. For clarity, only selected meteorite groups are shown (EC, enstatite chondrites; OC, ordinary chondrites; IAB, IAB iron meteorites); shaded areas represent ranges of bulk meteorites, where the widths of these areas correspond to the uncertainties on the CC and NC lines (see Fig. 1). Error bars typically represent 95% confidence intervals (95% CI).

The terrestrial rock samples show indistinguishable Mo isotopic compositions, averaging at $\varepsilon^{94}\text{Mo} = 0.04 \pm 0.06$ and $\varepsilon^{95}\text{Mo} = 0.10 \pm 0.04$ (95% CI) relative to the in-house Mo solution standard ($\varepsilon^{i}\text{Mo} \equiv 0$) (Supplementary Table 1). The small offset from zero most probably results from non-exponential isotopic fractionation induced during production of the high-purity standard, as has been observed for other elements[21,22]. As such, the terrestrial rock samples, and not the solution standards, are used to estimate the BSE's Mo isotopic composition (Supplementary Information).

The BSE's position among the NC and CC lines (Figs. 1 and 2) provides two first-order constraints on the nature of Earth's accreting material and how the provenance of this material evolved over time. First, because the BSE plots between the NC and CC lines, Earth must have accreted CC material during late stages of its growth; otherwise, the BSE would plot on the NC line. Second, no combination of known meteorites yields the BSE's Mo isotopic composition, indicating that Earth incorporated material that is distinct from known meteorites and enriched in *s*-process Mo. One possibility is that this *s*-process-enriched material derives from the NC reservoir, and the BSE's Mo isotopic composition reflects a mixture between this material and known CC material (Fig. 2b). However, the isotopic similarity of Earth and enstatite chondrites (EC) for many elements suggests that the average isotopic composition of Earth's accreting material was mostly similar to ECs[10]. As such, it is more likely that the *s*-process-enriched material derives from the CC reservoir, and the BSE's Mo isotopic composition reflects a mixture between this material and ECs (Fig. 2a). In this case, Earth's building material largely comprised objects with EC-like isotopic compositions[10], and isotopically distinct material was only added during late stages of accretion. The BSE's isotopic composition would then naturally be EC-like but would deviate preferentially for elements that were added late, such as Mo. For elements recording Earth's full accretion history (for example, Cr, Ti), the resulting changes would be small; assuming an EC-like isotopic composition for the proto-Earth, the addition of CC material during the last ~10% of accretion would have changed its ε^{54}Cr and ε^{50}Ti by only ~0.1–0.2, consistent with the small, albeit not resolved, difference between ECs and Earth for these two elements[18].

Regardless of such assumptions about the composition of Earth's building material, the relative contributions of NC and CC bodies to the BSE's Mo can be determined using the intercept theorem. As the NC and CC lines are parallel, the BSE composition divides any tie line between them into two segments whose ratio to each other is constant. Consequently, irrespective of the position of the endmembers on the NC and CC lines, the resulting mixing ratio between NC and CC material remains the same. Thus, unlike previous attempts[8–11,18], our approach for constraining the accretion of CC material to Earth is independent of the absolute isotope anomalies among Earth's accreting material.

To quantify the amount of CC material contributing to the BSE's Mo, we introduce the Δ^{95}Mo notation:

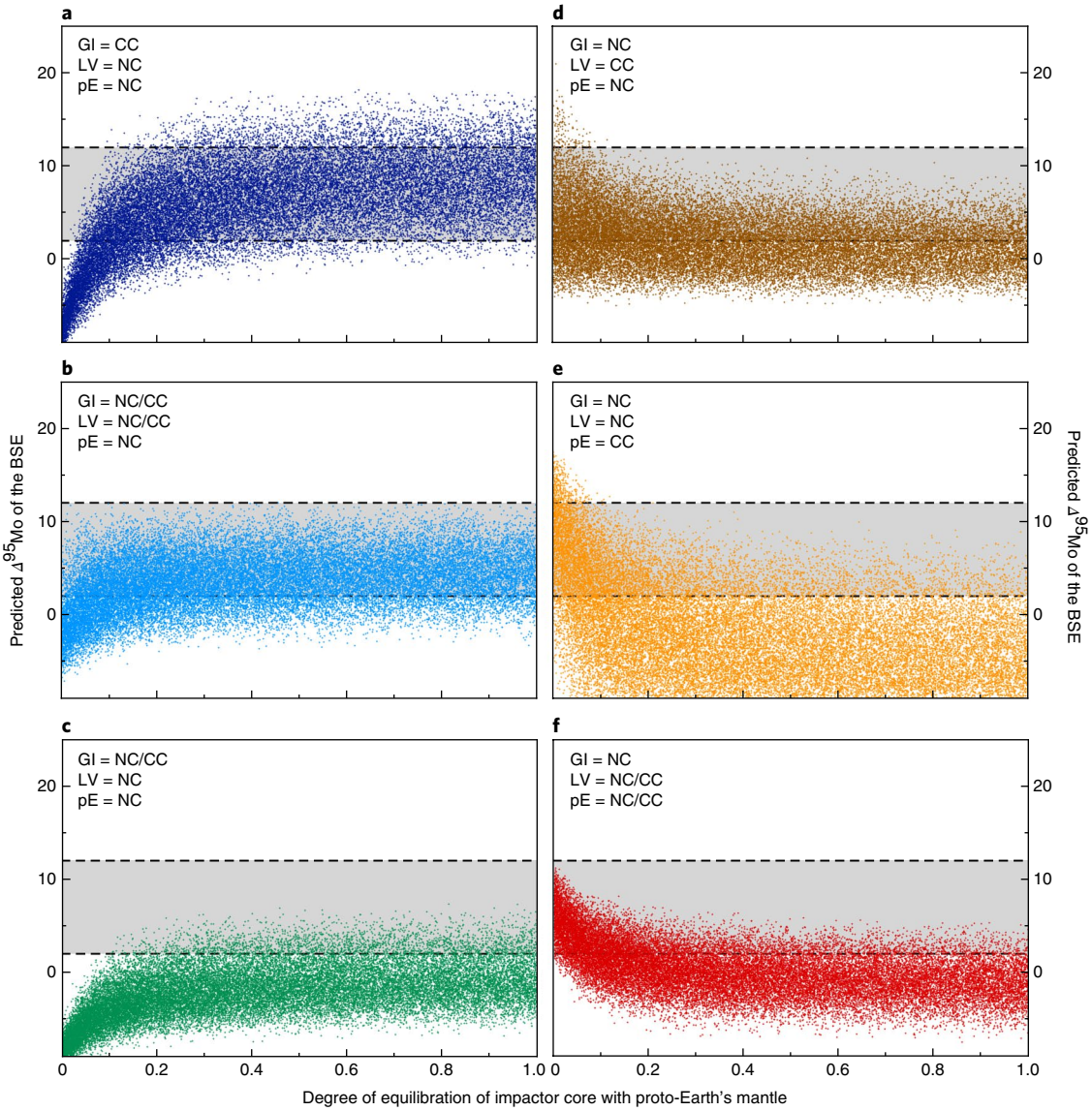

Fig. 3 | Predicted Δ^{95}Mo of the BSE versus the degree of impactor core re-equilibration during the Moon-forming impact. Grey horizontal bar represents the BSE's Δ^{95}Mo = 7 ± 5; dots represent outcomes of Monte Carlo simulations of the predicted Δ^{95}Mo resulting from mixing between proto-Earth's mantle (pE), the Moon-forming impactor (GI) and the late veneer (LV) of different compositions (Supplementary Information). **a**–**c**, A CC component in the Moon-forming impactor is assumed, while a pure NC composition is assumed for proto-Earth's mantle. **d**–**f**, A pure NC composition is assumed for the Moon-forming impactor, while a CC component is present in the late veneer and/or proto-Earth's mantle.

$$\Delta^{95}\mathrm{Mo} = (\varepsilon^{95}\mathrm{Mo} - 0.596 \times \varepsilon^{94}\mathrm{Mo}) \times 100 \quad (1)$$

where the slope of 0.596 represents the slope of the NC and CC lines; Δ^{95}Mo provides the parts-per-million deviation of any *s*-process mixing line from the origin and is a measure for the *r*-process excess relative to the composition of the Mo standard. For the NC and CC reservoirs we find $\Delta^{95}\mathrm{Mo_{NC}} = -9 \pm 2$ and $\Delta^{95}\mathrm{Mo_{CC}} = +26 \pm 2$ (Supplementary Information; Supplementary Fig. 1), which are unique isotope signatures for these two reservoirs, irrespective of the absolute isotope anomaly of a given sample. The mass fraction of CC-derived Mo (f_{CC}) in the present-day BSE is then given by mass balance:

$$f_{CC} = \frac{\Delta^{95}\mathrm{Mo_{BSE}} - \Delta^{95}\mathrm{Mo_{NC}}}{\Delta^{95}\mathrm{Mo_{CC}} - \Delta^{95}\mathrm{Mo_{NC}}} \quad (2)$$

From the terrestrial rock samples, we determined $\Delta^{95}\mathrm{Mo_{BSE}} = +7 \pm 5$ (Supplementary Information), corresponding to a mass fraction of CC-derived Mo in the BSE of 0.46 ± 0.15. Thus, ~30–60% of the BSE's Mo derives from the CC reservoir. Note that the total fraction of CC material in the bulk Earth is probably much smaller, because Mo records only the late stages of Earth's accretion.

As most of the BSE's Mo derives from the last 10–20% of accretion[10], its isotopic composition should be strongly influenced by the Moon-forming impactor, the last large body thought to collide with Earth[23], and by the late veneer, the material added to Earth's mantle after the giant impact and cessation of core formation[24]. To quantify the contribution of these components, we calculated the expected Δ^{95}Mo of the BSE for different assumed compositions of the Moon-forming impactor, the proto-Earth's mantle (Earth's mantle just before the giant impact), and the late veneer using a Monte Carlo approach (Supplementary Information). Several scenarios are considered in which pure CC, pure NC or mixed NC–CC (that is, a BSE-like Δ^{95}Mo of 7 ± 5) compositions are assumed for the three components (Fig. 3).

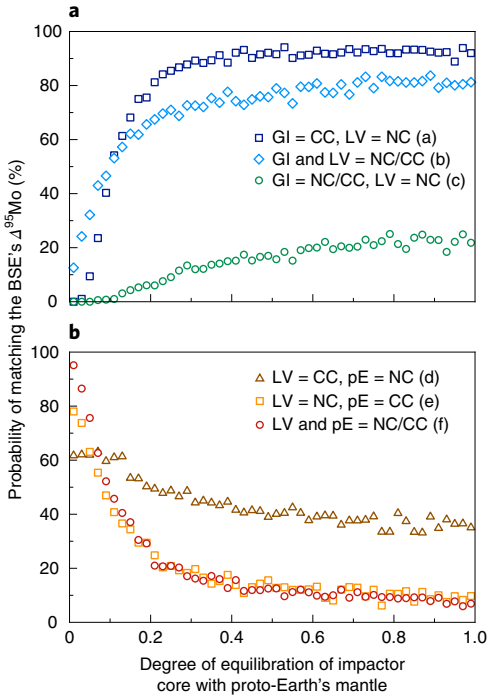

Fig. 4 | Probability of matching the BSE's Δ^{95}Mo for different compositions of proto-Earth's mantle (pE), the Moon-forming impactor (GI) and the late veneer (LV) as a function of impactor core re-equilibration during formation of the Moon. Probabilities calculated using the results from the modelling shown in Fig. 3. **a**, Probabilities for the scenarios in which the Moon-forming impactor always contains CC material (Fig. 3a–c). **b**, Probabilities for the scenarios in which the Moon-forming impactor always has a pure NC composition (Fig. 3d–f).

The BSE's Δ^{95}Mo is reproduced well when the Moon-forming impactor contains a significant amount of CC material (Fig. 4a). For instance, assuming a pure CC composition for the impactor reproduces the BSE's Δ^{95}Mo in >90% of the cases, provided that more than ~20% of the impactor core equilibrated with proto-Earth's mantle. For a mixed NC–CC composition of the Moon-forming impactor, the BSE's Δ^{95}Mo is reproduced in <20% of the cases, unless a mixed NC–CC composition is also assumed for the late veneer (Fig. 4a). By contrast, assuming a pure NC composition for the Moon-forming impactor provides the best match only for an impactor core re-equilibration of less than ~10% (Fig. 4b), because then most of the impactor's Mo is directly removed into Earth's core without contributing to the BSE's Mo. Although the degree of impactor core re-equilibration is poorly known, it was likely larger than ~40%[5,25]. Thus, there is only a small chance that the Moon-forming impactor had a pure NC composition; this holds true for all cases except if a pure CC composition for the late veneer is assumed (Fig. 4b). However, although Se/Te ratios[6] and Te isotopic compositions[26] suggest that the late veneer contained some CC material, the BSE's Ru and Os isotopic compositions are distinct from CC meteorites[8,27,28], demonstrating that the late veneer did not solely consist of CC bodies. Yet, assuming a mixed NC–CC composition for the late veneer does not provide a good match to the BSE's Δ^{95}Mo, even if a mixed NC–CC composition is also assumed for the proto-Earth's mantle (Fig. 4b). Thus, neither the late veneer nor the proto-Earth's mantle can be the sole source of CC material in the BSE. The CC material, therefore, was wholly or partly delivered by the Moon-forming impactor, which either had a pure CC or a mixed NC–CC composition.

A CC heritage of the Moon-forming impactor contrasts with the isotopic composition of the Moon itself, for which no CC signature has yet been found[22,29]. This implies that the Moon either formed from proto-Earth material[30,31] or equilibrated with Earth after the giant impact[32]. A CC heritage of the Moon-forming impactor also implies that, against current thinking[9,10], this body did not form in the inner Solar System but originated farther away, probably beyond Jupiter's orbit (that is, the presumed location of the CC reservoir[12,13]). Consistent with this, dynamical models of terrestrial planet formation predict that due to the orbital evolution of the gas giant planets—either during an early migration[33] or a later orbital instability[34]—embryos from beyond ~2.5 au were preferentially incorporated into Earth late, often with the final large impactor[2].

Assuming that the Moon-forming impactor had a pure CC composition and was Mars-sized[23], it would have added ~0.1 Earth masses of CC material. This amount would be lower if the impactor were smaller[31] or if it had a mixed NC–CC composition, which may have resulted from previous collisions between smaller NC and CC embryos. Nevertheless, although the Moon-forming impactor probably was not as volatile rich as CI chondrites, it still likely added the equivalent of 0.02 ± 0.01 Earth masses of CI material necessary to account for Earth's budget of water and highly volatile species[4].

Methods

Sample preparation and digestion of bulk meteorites and terrestrial samples. The meteorite samples investigated in the present study are summarized in Supplementary Table 1 and include different carbonaceous (CK, CH, CB) and Rumuruti chondrites as well as numerous groups of achondrites, such as acapulcoites, angrites, aubrites, brachinites, mesosiderites and ureilites (including two ureilitic fragments from the Almahata Sitta meteorite named MS-MU-17 and MS-MU-20), as well as the ungrouped achondrites Tafassasset and NWA 1058. For almost all of these groups of meteorites no high-precision Mo isotopic data have been reported before.

Pieces of these meteorites (~0.3–2 g) were carefully cleaned by polishing with SiC as well as sonication in ethanol, and then ground to a fine powder in an agate mortar. Since bulk aubrites have very low Mo concentrations (~10 ppb), an ~10.5 g piece of Peña Blanca Spring and ~0.5 g of a metal nodule from Norton County were used. Bulk meteorite samples as well as terrestrial rock standards were digested in Savillex vials on a hotplate using HF–HNO_3–$HClO_4$ (2:1:0.01) at 180–200 °C (5 days), followed by inverse aqua regia (2:1 HNO_3–HCl) at 130–150 °C (2 days) and repeated dry-downs with 6 M HCl–0.06 M HF.

Leaching procedure for ordinary chondrites. Pieces of the unequilibrated ordinary chondrites NWA 2458 (L3.2; 6.48 g) and WSG 95300 (H3.3; 4.35 g) were carefully cleaned by polishing with SiC as well as sonication in ethanol, and then ground to a fine powder in an agate mortar. Thereafter, these powders were subjected to a sequential (six-step) leaching procedure in Savillex vials as summarized in Supplementary Table 3, which was modified from ref. [35]. Only ultrapure water (Milli-Q) and twice-distilled (HCl, HNO_3, HF) or 'suprapur' (HAc, $HClO_4$) acids were used, and a blank was processed through the entire leaching procedure together with the two samples. In addition to the acid leachates, a whole rock sample of NWA 2458 was also analysed (as described above).

After each leaching step, the samples were centrifuged at 4,400 r.p.m. (~2,900*g*) for 30 min and the supernatant was separated from the precipitate. The precipitate was rinsed 4–5 times with 5–10 ml H_2O to remove the remaining acid, where each rinse step was followed by centrifuging and separating the rinse from the precipitate. All rinse steps were combined with the corresponding supernatant to the final leachate, and the remaining precipitate was then subjected to the next leaching step. Note that after sub-step L6a (HF–HNO_3–$HClO_4$), the samples were dried down and $HClO_4$ was removed by repeated dry-downs with HNO_3 at 180–200 °C before adding inverse aqua regia (L6b). After sub-step L6b, the samples were centrifuged (see above), leaving behind a small amount of insoluble residue that was not further investigated.

At this stage, small aliquots (~2%) of all leachates were taken to determine Mo contents. The aliquots were dried down, treated with inverse aqua regia to attack organics, and dissolved in 0.5 M HNO_3–0.01 M HF. Mo contents were then measured on a Thermo Scientific XSeries 2 quadrupole inductively coupled plasma mass spectrometer (ICP-MS). Depending on the amount of Mo present, 30–90% splits of the leachates were used for the Mo isotope composition analyses. These were dried down and treated with inverse aqua regia to attack organics, followed by repeated dry-downs with 6 M HCl–0.06 M HF.

Chemical separation of Mo. The chemical separation of Mo was accomplished following the analytical protocol described in refs. [12,36]. First, Mo was separated from most of the sample matrix using a two-stage anion exchange chromatography. In the first stage, the samples were typically loaded in 75 ml 0.5 M HCl–0.5 M HF onto columns filled with 4 ml of pre-cleaned Bio-Rad AG1-X8 anion exchange

resin (200–400 mesh). Most of the sample matrix was washed off the columns with the loading solution and additional 10 ml 0.5 M HCl–0.5 M HF. The high-field-strength elements (HFSE) and W were then eluted in 15 ml 6 M HCl–1 M HF, while Mo largely (~85%) remained on the resin, and was subsequently collected using 10 ml 3 M HNO_3. To prevent overloading the columns, samples of more than ~0.5 g (for example, ureilites, NWA 4931, L1/L2/L6 leachates) were dissolved in 150–300 ml 0.5 M HCl–0.5 M HF and then processed consecutively in 2–4 splits (equivalent to ~0.5 g sample each) through the first anion exchange chromatography (the same column and resin were re-used for all splits of the same sample, and both the HFSE and the Mo cuts from the different splits were re-combined afterwards). The Peña Blanca Spring sample (~10.5 g) was loaded in a total of 1,500 ml 0.5 M HCl–0.5 M HF and processed as described above, albeit using several columns (20 splits). Note that this procedure neither affected the total yield nor the accuracy of the isotope data, which is demonstrated by the Mo isotope composition of the Peña Blanca Spring sample being indistinguishable from that of the Norton County metal nodule.

A small fraction (~15%) of the Mo is typically eluted together with the HFSEs. This Mo was recovered during the second stage, where all samples were loaded in 6 ml 0.6 M HF–0.4% H_2O_2 onto Bio-Rad Poly-Prep columns containing 1 ml of pre-cleaned AG1-X8 resin (200–400 mesh). The columns were then rinsed with 10 ml 1 M HCl–2% H_2O_2, 9 ml 8 M HCl–0.01 M HF, 0.5 ml 6 M HCl–1 M HF, and 8.5 ml 6 M HCl–1 M HF to quantitatively remove the HFSEs, followed by elution of Mo with 5 ml 3 M HNO_3.

The Mo cuts from both stages were then combined, and Mo concentrations as well as the purity of the samples were determined on small aliquots (equivalent to ~5 ng Mo) of the combined Mo cuts by quadrupole ICP-MS. At this stage, samples with high Fe/Mo (for example, ureilites, L1/L6 leachates), Ru/Mo (L2 leachates) or Nb/Mo (JA-2, JG-1, W-2a) were further purified with an additional anion exchange chromatography, which was slightly modified from ref. [37]. For the clean-up, the respective samples were loaded in 7 ml 1 M HF onto Bio-Rad Poly-Prep columns containing 2 ml of pre-cleaned AG1-X8 resin (100–200 mesh). The columns were then rinsed with 14 ml 1 M HF, 20 ml 6 M HCl–0.06 M HF and 8 ml 6 M HCl–1 M HF to quantitatively remove Fe, Ru, and remaining HFSE (particularly Nb) from the Mo cuts.

The final purification of Mo was performed using a two-stage ion exchange chromatography that was slightly modified from ref. [37]. The samples were loaded in 1 ml 1 M HCl onto columns filled with 1 ml pre-cleaned Eichrom TRU Resin (100–150 µm) and, after rinsing with 6 ml 1 M HCl, Mo was eluted in 6 ml 0.1 M HCl. This chemistry was repeated once, but using 7 M HNO_3 and 0.1 M HNO_3 instead of 1 M HCl and 0.1 M HCl, respectively. The Mo cuts from all ion chromatography steps were evaporated with added HNO_3 and inverse aqua regia to destroy organic compounds. The Mo yield for the entire procedure was typically ~75%, and total procedural blanks were typically ~2–4 ng Mo and thus negligible. Only for the L6 leachates the blank of ~11 ng was significant and required a small blank correction of ~1ε on ε^{92}Mo. We note, however, that this blank correction has no effect on the interpretation of the Mo isotope data, particularly the ε^{95}Mo–ε^{94}Mo systematics.

Mo isotope measurements. The Mo isotope compositions were measured on a Thermo Scientific Neptune Plus multicollector inductively coupled plasma mass spectrometer (MC-ICP-MS) in the Institut für Planetologie at the University of Münster, and followed the measurement protocol described in refs. [12,36]. Sample solutions were introduced into the mass spectrometer using a self-aspirating Savillex C-Flow PFA nebulizer (~50 µl min^{-1} uptake rate) connected to a Cetac Aridus II desolvator. The measurements were performed in low-resolution mode using standard Ni sampler and (H) skimmer cones, which yielded total ion beam intensities of ~1.1×10^{-10} A for a ~100 ppb Mo solution. Each measurement consisted of 40 baseline integrations (on-peak zeros) of 8.4 s each followed by 100 Mo isotope ratio measurements of 8.4 s each, which consumed ~80 ng of Mo. All data were corrected for instrumental mass bias by internal normalization to $^{98}Mo/^{96}Mo = 1.453173$ using the exponential law, because this normalization results in large Mo isotope anomalies and distinctive isotope patterns[37]. Small isobaric interferences of Zr and Ru on Mo masses were corrected by monitoring interference-free ^{91}Zr and ^{99}Ru. The final Mo cuts typically had Ru/Mo and Zr/Mo of $<1\times10^{-4}$, where the interference corrections for Ru (on ε^{100}Mo) and Zr (on ε^{94}Mo) were always $<2\varepsilon$, respectively. Note that Zr interference corrections of up to ~25ε (Zr/Mo ≈ 1.4×10^{-3}) and Ru interference corrections of >20ε (Ru/Mo ≈ 2.1×10^{-3}) are accurate to within analytical uncertainty[12].

The Mo isotope ratios are reported as ε^iMo values, which represent the parts-per-10,000 deviation of a sample from the mean of the bracketing runs of the Alfa Aesar solution standard, where $\varepsilon^i\mathrm{Mo} = [(^i\mathrm{Mo}/^{96}\mathrm{Mo})_{\mathrm{sample}} / (^i\mathrm{Mo}/^{96}\mathrm{Mo})_{\mathrm{standard}} - 1]\times10^4$ (i = 92, 94, 95, 97, 100). For samples analysed multiple times, the reported ε^iMo values represent the mean of pooled solution replicates together with their associated external uncertainties. The external reproducibility of the Mo isotope measurements ranges from ±0.15 for ε^{97}Mo to ±0.35 for ε^{92}Mo (2s.d.), as defined by repeated analyses of the BHVO-2 rock standard, several digestions of which were processed through the full analytical procedure and analysed together with each set of samples (Supplementary Table 2).

Since some previous studies reported Mo isotope data relative to different solution standards, we measured the composition of the NIST SRM 3134 (for example, ref. [14]) and Alfa Aesar Specpure Plasma (for example, refs. [11,15]) standards relative to the Alfa Aesar solution standard used in the Institut für Planetologie at the University of Münster. Repeated analyses of these standards during multiple measurement sessions demonstrate that all these solution standards have indistinguishable Mo isotopic compositions (Supplementary Table 1). Furthermore, to demonstrate the accuracy of our procedure, we processed our Alfa Aesar and the NIST SRM 3134 solution standards as well as different digestions of the DTS-2b rock standard that were doped with our Alfa Aesar standard (DTS-2b is extremely depleted in Mo and thus >90% of the measured mixture is from the Alfa Aesar standard) through the full analytical protocol described above. All processed solution standards are indistinguishable from the unprocessed solution standards (Supplementary Table 1), demonstrating that the chemical separation does not induce any resolvable effects on the measured Mo isotope compositions.

Data availability

All data generated during this study are included in this article (and its Supplementary Information files).

Received: 11 December 2018; Accepted: 9 April 2019;
Published online: 20 May 2019

References

1. Morbidelli, A., Lunine, J. I., O'Brien, D. P., Raymond, S. N. & Walsh, K. J. Building terrestrial planets. *Annu. Rev. Earth Planet. Sci.* **40**, 251–275 (2012).
2. O'Brien, D. P., Izidoro, A., Jacobson, S. A., Raymond, S. N. & Rubie, D. C. The delivery of water during terrestrial planet formation. *Space Sci. Rev.* **214**, 47 (2018).
3. Alexander, C. M. O'D. et al. The provenances of asteroids, and their contributions to the volatile inventories of the terrestrial planets. *Science* **337**, 721–723 (2012).
4. Marty, B. The origins and concentrations of water, carbon, nitrogen and noble gases on Earth. *Earth Planet. Sci. Lett.* **313-314**, 56–66 (2012).
5. Rubie, D. C. et al. Accretion and differentiation of the terrestrial planets with implications for the compositions of early-formed Solar System bodies and accretion of water. *Icarus* **248**, 89–108 (2015).
6. Wang, Z. & Becker, H. Ratios of S, Se and Te in the silicate Earth require a volatile-rich late veneer. *Nature* **499**, 328–331 (2013).
7. Albarede, F. Volatile accretion history of the terrestrial planets and dynamic implications. *Nature* **461**, 1227–1233 (2009).
8. Fischer-Gödde, M. & Kleine, T. Ruthenium isotopic evidence for an inner Solar System origin of the late veneer. *Nature* **541**, 525–527 (2017).
9. Schiller, M., Bizzarro, M. & Fernandes, V. A. Isotopic evolution of the protoplanetary disk and the building blocks of Earth and the Moon. *Nature.* **555**, 507–510 (2018).
10. Dauphas, N. The isotopic nature of the Earth's accreting material through time. *Nature* **541**, 521–524 (2017).
11. Bermingham, K. R., Worsham, E. A. & Walker, R. J. New insights into Mo and Ru isotope variation in the nebula and terrestrial planet accretionary genetics. *Earth Planet. Sci. Lett.* **487**, 221–229 (2018).
12. Budde, G. et al. Molybdenum isotopic evidence for the origin of chondrules and a distinct genetic heritage of carbonaceous and non-carbonaceous meteorites. *Earth Planet. Sci. Lett.* **454**, 293–303 (2016).
13. Kruijer, T. S., Burkhardt, C., Budde, G. & Kleine, T. Age of Jupiter inferred from the distinct genetics and formation times of meteorites. *Proc. Natl Acad. Sci. USA* **114**, 6712–6716 (2017).
14. Poole, G. M., Rehkämper, M., Coles, B. J., Goldberg, T. & Smith, C. L. Nucleosynthetic molybdenum isotope anomalies in iron meteorites—new evidence for thermal processing of solar nebula material. *Earth Planet. Sci. Lett.* **473**, 215–226 (2017).
15. Worsham, E. A., Bermingham, K. R. & Walker, R. J. Characterizing cosmochemical materials with genetic affinities to the Earth: genetic and chronological diversity within the IAB iron meteorite complex. *Earth Planet. Sci. Lett.* **467**, 157–166 (2017).
16. Burkhardt, C. et al. A nucleosynthetic origin for the Earth's anomalous ^{142}Nd composition. *Nature* **537**, 394–398 (2016).
17. Render, J., Fischer-Gödde, M., Burkhardt, C. & Kleine, T. The cosmic molybdenum-neodymium isotope correlation and the building material of the Earth. *Geochem. Persp. Lett.* **3**, 170–178 (2017).
18. Warren, P. H. Stable-isotopic anomalies and the accretionary assemblage of the Earth and Mars: a subordinate role for carbonaceous chondrites. *Earth Planet. Sci. Lett.* **311**, 93–100 (2011).
19. Nicolussi, G. K. et al. Molybdenum isotopic composition of individual presolar silicon carbide grains from the Murchison meteorite. *Geochim. Cosmochim. Acta* **62**, 1093–1104 (1998).
20. Nanne, J. A. M., Nimmo, F., Cuzzi, J. N. & Kleine, T. Origin of the non-carbonaceous–carbonaceous meteorite dichotomy. *Earth Planet. Sci. Lett.* **511**, 44–54 (2019).

21. Steele, R. C. J., Elliott, T., Coath, C. D. & Regelous, M. Confirmation of mass-independent Ni isotopic variability in iron meteorites. *Geochim. Cosmochim. Acta* **75**, 7906–7925 (2011).
22. Zhang, J. J., Dauphas, N., Davis, A. M., Leya, I. & Fedkin, A. The proto-Earth as a significant source of lunar material. *Nat. Geosci.* **5**, 251–255 (2012).
23. Canup, R. M. & Asphaug, E. Origin of the Moon in a giant impact near the end of the Earth's formation. *Nature* **412**, 708–712 (2001).
24. Walker, R. J. Highly siderophile elements in the Earth, Moon and Mars: update and implications for planetary accretion and differentiation. *Chem. Erde-Geochem.* **69**, 101–125 (2009).
25. Rudge, J. F., Kleine, T. & Bourdon, B. Broad bounds on Earth's accretion and core formation constrained by geochemical models. *Nat. Geosci.* **3**, 439–443 (2010).
26. Fehr, M. A., Hammond, S. J. & Parkinson, I. J. Tellurium stable isotope fractionation in chondritic meteorites and some terrestrial samples. *Geochim. Cosmochim. Acta* **222**, 17–33 (2018).
27. Bermingham, K. R. & Walker, R. J. The ruthenium isotopic composition of the oceanic mantle. *Earth Planet. Sci. Lett.* **474**, 466–473 (2017).
28. Meisel, T., Walker, R. J. & Morgan, J. W. The osmium isotopic composition of the Earth's primitive upper mantle. *Nature* **383**, 517–520 (1996).
29. Akram, W. & Schönbächler, M. Zirconium isotope constraints on the composition of Theia and current Moon-forming theories. *Earth Planet. Sci. Lett.* **449**, 302–310 (2016).
30. Canup, R. M. Forming a Moon with an Earth-like composition via a giant impact. *Science* **338**, 1052–1055 (2012).
31. Cuk, M. & Stewart, S. T. Making the Moon from a fast-spinning Earth: a giant impact followed by resonant despinning. *Science* **338**, 1047–1052 (2012).
32. Lock, S. J. et al. The origin of the Moon within a terrestrial synestia. *J. Geophys. Res.* **123**, 910–951 (2018).
33. O'Brien, D. P., Walsh, K. J., Morbidelli, A., Raymond, S. N. & Mandell, A. M. Water delivery and giant impacts in the 'Grand Tack' scenario. *Icarus* **239**, 74–84 (2014).
34. O'Brien, D. P., Morbidelli, A. & Levison, H. F. Terrestrial planet formation with strong dynamical friction. *Icarus* **184**, 39–58 (2006).
35. Reisberg, L. et al. Nucleosynthetic osmium isotope anomalies in acid leachates of the Murchison meteorite. *Earth Planet. Sci. Lett.* **277**, 334–344 (2009).
36. Budde, G., Kruijer, T. S. & Kleine, T. Hf-W chronology of CR chondrites: implications for the timescales of chondrule formation and the distribution of ^{26}Al in the solar nebula. *Geochim. Cosmochim. Acta* **222**, 284–304 (2018).
37. Burkhardt, C. et al. Molybdenum isotope anomalies in meteorites: constraints on solar nebula evolution and origin of the Earth. *Earth Planet. Sci. Lett.* **312**, 390–400 (2011).

Acknowledgements

We are grateful to NASA and the Institute of Meteoritics, University of New Mexico, for providing samples. We are also grateful to K. Metzler, G. Brennecka and A. Bischoff for discussions, C. Brennecka for comments on the paper, U. Heitmann for technical support, as well as R. Walker and K. Bermingham (University of Maryland) for providing their Mo solution standard. This study was supported by the European Research Council Consolidator Grant "ISOCORE" (contract 616564) and by the Deutsche Forschungsgemeinschaft (SFB/TRR 170 subproject B3-1). This is TRR publication no. 61.

Author contributions

G.B., C.B. and T.K. devised the study. G.B. prepared the samples for Mo isotope analyses and performed all measurements. All authors contributed to the interpretation of the data and preparation of the manuscript.

Competing interests

The authors declare no competing interests.

Additional information

Supplementary information is available for this paper at https://doi.org/10.1038/s41550-019-0779-y.

Reprints and permissions information is available at www.nature.com/reprints.

Correspondence and requests for materials should be addressed to G.B.

Publisher's note: Springer Nature remains neutral with regard to jurisdictional claims in published maps and institutional affiliations.

© The Author(s), under exclusive licence to Springer Nature Limited 2019